Liquid Crystals
Publication details, including instructions for authors and subscription information:
http://www.informaworld.com/smpp/title~content=t713926090

A study of the transition of liquid-crystal alignment from homeotropic to planar on a polyimide layer

Jian Wang[a]; Lei Wang[a]; Yu Zeng[a]; Yu-Qing Fang[a]; Qin Zhang[a]; Yinghan Wang[a]
[a] State Key Laboratory of Polymer Materials Engineering of China, College of Polymer Science and Engineering, Sichuan University, Chengdu, China

Online publication date: 04 March 2010

To cite this Article Wang, Jian , Wang, Lei , Zeng, Yu , Fang, Yu-Qing , Zhang, Qin and Wang, Yinghan(2010) 'A study of the transition of liquid-crystal alignment from homeotropic to planar on a polyimide layer', Liquid Crystals, 37: 3, 271 — 278
To link to this Article: DOI: 10.1080/02678290903443905
URL: http://dx.doi.org/10.1080/02678290903443905

Liquid Crystals,
Vol. 37, No. 3, March 2010, 271–278

Taylor & Francis
Taylor & Francis Group

A study of the transition of liquid-crystal alignment from homeotropic to planar on a polyimide layer

Jian Wang, Lei Wang, Yu Zeng, Yu-Qing Fang, Qin Zhang and Yinghan Wang*

State Key Laboratory of Polymer Materials Engineering of China, College of Polymer Science and Engineering, Sichuan University, Chengdu 610065, China

(Received 18 August 2009; accepted 26 October 2009)

The alignment of nematic liquid crystals by rubbed polyimide surfaces has been well-studied and developed. A novel polyimide film which induced a homeotropic alignment of the nematic liquid crystal without rubbing or with weak rubbing strength was presented. However, there was a transition from homeotropic to planar alignment of the nematic liquid crystal after strong rubbing. In order to study the transition, the polyimide surface was investigated by atomic force microscopy, surface free energy measurement and angle-resolved analysis X-ray photo-electron spectroscopy before and after rubbing with a velvet fabric. It was found that both the change of surface polarity and surface morphology were not the reasons for the transition. The droop of the side chain on the polyimide surface after the rubbing treatment was detected by angle-resolved analysis X-ray photo-electron spectroscopy. Owing to the special structure of the novel polyimide, the X-ray photo-electron spectroscopy was successfully used for the first time to analyse the conformational change of the side chain of a polymer. In conclusion, the transition of nematic liquid crystal alignment from homeotropic to planar after rubbing was influenced by the side chain conformation of the polyimide.

Keywords: polyimide; side chain; vertical alignment; liquid crystal; transition

1. Introduction

The alignment of a nematic liquid crystal (NLC), consisting of an assembly of rod-like molecules, on rubbed polyimide (PI) surfaces underlies the manufacture of today's flat panel displays. Although many new-style alignment methods have been proposed, such as photo-alignment, ion beam alignment, hierarchical self-assembly and so on [1–3], rubbed-PI is still the predominant technology among all the methods due to its comprehensively excellent performance.

The pretilt angle prevents the creation of disclinations in LC cells and is also very necessary in the prevention of stripe domains in liquid crystal displays (LCDs). Recently, several new LCD modes have been introduced to overcome the problems of traditional twisted nematic LCDs, which are low contrast ratio, slow response time and narrow view angle. Most of these new LCD modes utilise vertical alignment for NLCs, such as continuous pinwheel alignment, multi-domain vertical alignment and patterned vertical alignment. A stable pretilt angle for vertical alignment is necessary and very important for these LCD modes. Although some investigations on the change of pretilt angles for homeotropic alignment of NLCs on rubbed PI have been reported [4–6], there is still a lack of deep understanding with respect to surface chemical and physical structures for change of the pretilt angle. In recent years, the control of pretilt angle of LC molecules for planar alignment has been intensively investigated [7–13]. It was pointed out that both surface polarity and the side chains of a polymer have a vital influence on the pretilt angle of NLCs, that is, the pretilt angles become larger with decrease of surface polarity and the introduction of side chains on a PI. Lately, Da-Ren *et al.* [14, 15] reported that an increase of groove depth could cause a transition of NLC alignment from homeotropic to planar. It was suggested that surface morphology also has a remarkable influence on the pretilt angle of homeotropic NLC alignment. From these studies it is clear that the pretilt angle can be influenced by various factors.

On the other hand, according to the use of near-edge X-ray absorption fine structure spectroscopy (NEXAFS), sum frequency generation (SFG), second-harmonic generation (SHG) and sum-frequency generation vibrational spectroscopy [16–19] for investigating the molecular conformation on polymer surface layers, some researchers attempted to elucidate the mechanism of the NLC pretilt angle and molecular alignment. However, so far no clear explanation has been found for the correlation between the molecular conformation of alignment layers and NLC pretilt angles due to the complexity and variety of PI surface chemical and physical structures.

In a previous report, we described the synthesis of a novel PI, which can induce NLC vertical alignment

*Corresponding author. Email: prof_wangpaper@126.com

ISSN 0267-8292 print/ISSN 1366-5855 online

DOI: 10.1080/02678290903443905
http://www.informaworld.com

[20]. It was found that there is a transition of the LC alignment from homeotropic to planar with an increase in rubbing strength. In order to study more deeply the transition on the PI alignment layer and to clarify the correlation between surface chemical and physical structures of the alignment and NLC pretilt angles, it is necessary to analyse the factors that can influence the pretilt angle of NLCs. In this study, we focused on the specifically designed aromatic PI containing pendent bulky mesogens as an alignment layer having a vertical alignment for NLCs. According to particular investigations, we discuss the reasons for the transition from homeotropic alignment to planar on the PI layer after a strong rubbing process.

2. Experimental

2.1 Materials and fabrication of PI films

In this experiment, the PI for homeotropic alignment was used. The chemical structure is shown in Figure 1. Glass substrates were cleaned with sodium hydroxide solution, distillation water and isopropanol rinses in ultrasonic baths. Mica substrates were prepared by cleaving the top layers from a mica slide with tape to provide a clean surface. Poly (amic acid)s at a solid content of 5 wt% in N-methyl-2-pyrrolidone were spin-coated on the clean glass or mica substrates at 600 rpm for 15 s and 2300 rpm for 30 s. The coated films were pre-baked at 100°C for 20 min and cured at 230°C for 30 min, which produced the PI films. The films surfaces were rubbed with a velvet fabric using a rubbing machine to obtain rubbed samples. The rubbing strength (RS) has been defined in a previous paper [21]. Some LC cells were assembled with two pieces of rubbed substrates in an antiparallel rubbing direction; other NLC cells were assembled with two pieces of the non-rubbed substrates using a 40 μm-thick adhesive film spacer. An NLC (5CB) was injected into a cell gap using a capillary method. As shown in Figure 2, the transition of alignment from homeotropic to planar in an LC cell occurred between RS = 230 mm and RS = 330mm.

2.2 Characterization methods

Surface images were obtained with a tapping mode atomic force microscope (AFM) (Explorer SPM, Vecco Instruments, Plainview, NY, USA). The rubbing process was operated with a rubbing machine from TianLi Co. Ltd (Chengdu, China). The spin-coating process was executed using a KW-4A spinner from the Institute of Microelectronics of the Chinese Academy of Science (Peking, China). The pretilt angles of LCs were measured by a crystal rotation method using a pretilt angle tester from the Changchun Institute of Optics. Polarising microscopy from Shanghai Millimeter Precision Instrument Co. Ltd (Shanghai, China) was used to evaluate the alignment behaviour of the LCs. Contact angles were measured by the sessile drop method using a contact anglemeter (DSA100, Kruss, Hamburg, Germany), and the surface free energy was calculated by Owens's formula. The X-ray photo-electron spectroscope (XPS) measurements of the samples were performed at room temperature with an XSAM800 Kratos instrument system employing monochromatic Mg K-alpha X-ray radiation (1253.6 eV), the operating pressure during analysis was in the low 10^{-9} torr range. The reference binding energy was set at 284.6 eV for the C–C and C–H components of the C ls core level

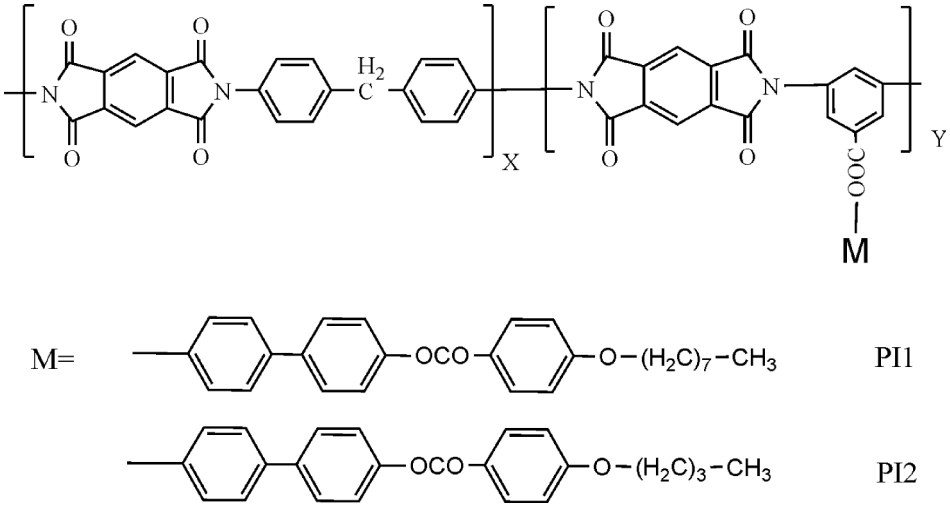

Figure 1. Chemical structure of the polyimides.

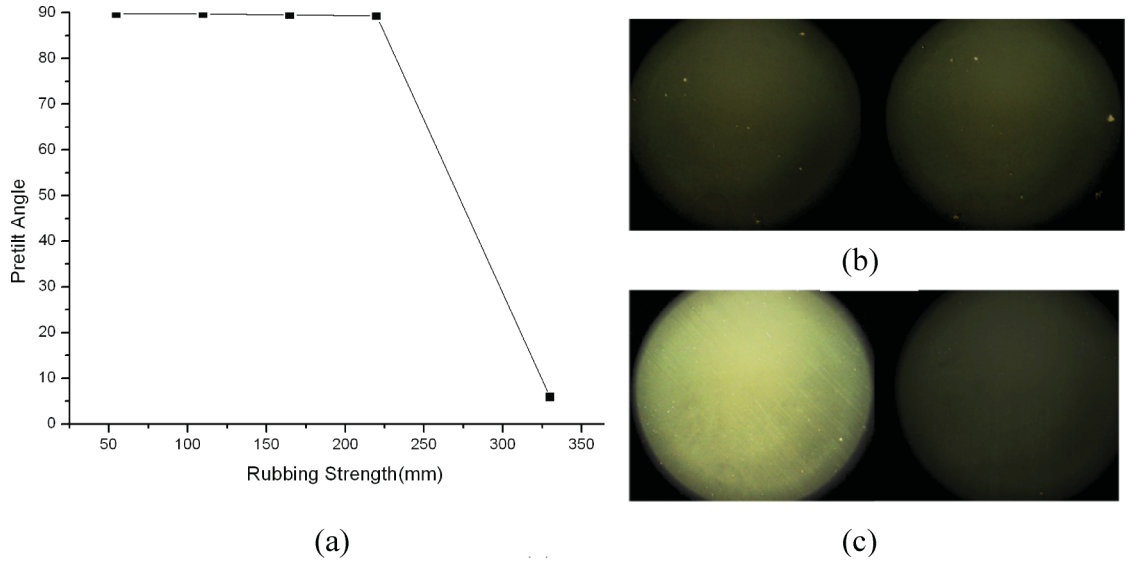

Figure 2. (a) Pretilt angles of 5CB on the rubbed polyimide I surface as a function of rubbing strength (RS); transition of liquid-crystal (LC) alignment from homeotropic to planar take place between RS = 230 mm and 330 mm. (b) Polarising optical micrographs of nematic liquid crystal (NLC) alignment in an LC cell (RS = 230 mm). (c) Polarising optical micrographs of NLC alignment in an LC cell. (RS = 330 mm). The optical micrographs on the right-hand side are taken by rotating the stage by 45° relative to that of the left-hand side.

spectra. Atomic concentrations were calculated using XPS peak software (version 3.1). The energy-minimised structures of the PIs were calculated using Materials Studio 4.0 (Accelrys Inc.).

3. Results and discussion

3.1 Surface free energy

The surface free energy was investigated for the PI films to analyse quantitatively the change of surface polarity of the polymer after the rubbing process. In Table 1, polar forces occupy a very small proportion of the total surface free energy due to the alkyl side chain orientation out of the plane of the surface masking the polar imide group [22]. It was seen that there is little change of the total surface free energy and dispersion force on the surface. However, polar forces increase more than two times after the rubbing process, which suggests that polar groups increase significantly on the PI surface by means of very strong rubbing. The change of polar force is more significant than that of PIs by common rubbing strength [23]. It is well known that surface polarity has an important influence on the pretilt angle of an NLC. In this case, in order to clarify the influence of surface free energy on NLC alignment, we decreased the alkyl carbon number of the side chain tail end to help in analysing the change of surface free energy (Figure 3). The decrease of the alkyl carbon number not only increased the polar group proportion of the PI surface, but also remained the same chemical structure. Thus PI2 was introduced and synthesised and the chemical structure is shown in Figure 1. The unrubbed PI2 film could induce vertical alignment for the NLC and the pretilt angle of the NLC for weakly rubbed PI2 (RS = 55 mm) is still above 89°. On the other hand, it can be seen that both polar force and surface free energy on the PI2 surface is larger than that of PI1, which suggests the increase of the polar group on the surface

Table 1. Polarity of surface with respect to polyimide 1 and polyimide 2.

	Unrubbed polyimide 1 (dyn cm^{-2})	Rubbed polyimide 1 (rubbing strength = 330 mm, dyn cm^{-2})	Unrubbed polyimide 2 (dyn cm^{-2})	Rubbed polyimide 2 (rubbing strength = 165 mm, dyn cm^{-2})
Disperse force	39.48	41.06	40.56	40.73
Polar part	1.99	4.24	5.23	6.05
Total surface free energy	41.47	44.8	45.79	46.78

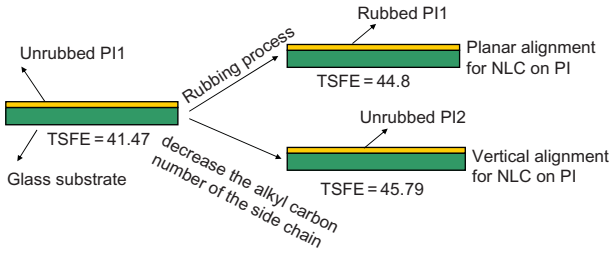

Figure 3. A schematic method for estimating the influence of surface free energy on nematic liquid crystal alignment. TSFE = total surface free energy.

resulting from a strong rubbing process actually cannot induce the change of NLC alignment from homeotropic to planar on a PI layer.

Moreover, after a relatively weak rubbing process (RS = 165 mm), the alignment transition from homeotropic to planar on PI2 could take place, and the pretilt angle of an LC for PI2 is 6.4°. It can be concluded that the occurrence of the transition on PI2 is easier than PI1, which suggests that the decrease of the flexible carbon chain obviously reduces the rubbing resistance of vertical alignment. The change of PI2 surface free energy after rubbing is also shown in Table 1. It can be seen that the polar force and total surface free energy only increase slightly, which also implies that the transition is not caused by the change of surface polarity.

3.2 *Surface morphology*

Using the AFM, the surface of the PI films was examined before and after a strong rubbing process. Figure 4(a) shows the surface morphology of pristine PI1 films. The root-mean-square (RMS) roughness is 0.46 nm over an area of $2.5\times2.5\ \mu m^2$. The film surface is apparently covered with sub-micrometre-scaled spikes (see Figure 4(a)).The surface morphology and roughness of the PI film derive mainly from the characteristics of the polymer chains that govern the aggregation and molecular ordering that occur during the drying and thermal imidisation processes after spin-casting [24]. Figure 4(b) shows the surface morphology of PI1 after a strong rubbing process. The RMS roughness is 0.49 nm over an area of $2.5\times2.5\ \mu m^2$. It was noticed that the roughness on the PI films almost did not change after the rubbing process. The phenomenon is abnormal, because the roughness is usually subjected to notable change after strong rubbing. Moreover, it can be seen that the surface seems smoother due to the disappearance of the sub-microgrooves (Figure 4(b)), which can be observed clearly in Figure 4(a). The disappearance of sub-microgrooves reduces the change of roughness. The reason for the sub-microgrooves disappearance is still unknown and needs further investigation, but molecular rearrangement of the PI surface probably induces the disappearance of the sub-microgrooves. Mada and Snoda [25] suggested that the temperature of the hot spots caused by textile buffing can briefly rise to 230°C, which is close to the glass transition temperature (T_g) of PI. Toney [26] suggested that the T_g of the surface is lower than that of the bulk, and the reorientation might have occurred at the lower temperatures. As far as the novel PI is concerned, the bulky aryl rigid side chain tends to push the alkyl flexible side chain outwards off the main chain, thereby a lot of alkyl congregates on the PI surface, which further reduces the T_g of the PI surface and easily causes the molecular reorientation and movement.

On the other hand, Da-Ren *et al.* [15, 16] have demonstrated that the increase of groove depth on PI films can decrease the pretilt angle, however, in our case it is evident that groove depth did not visibly increase. The depth of the microgrooves was less than 3 nm for both rubbed and unrubbed PIs. Although we cannot exclude the possibility that the disappearance of the sub-microgroove had an effect on the pretilt angle of the LC, the tiny change in morphology of the surface is unlikely to induce the transition of NLC alignment from homeotropic to planar. Thus, it is concluded that the surface morphology cannot influence the transition.

3.3 *Side chain conformation*

We calculated the conformation of the PI molecule by the Discover Module of the Materials Studio software. The Compass fore field was used in this case. As shown in Figure 5, according to energy minimising and molecular dynamic simulation, we can calculate the optimised conformation of the PI. The side chain of the pristine PI1 is almost perpendicular to the main chain, and the rigid side chain on the surface is easily oriented outwards in the polymer bulk phase, which results in low surface energy and an enrichment of the non-polar alkyl side chain at the outmost layer of the PI surface. Some investigations [17, 19] also indicate that the side chain outward orientation is important for the LC molecule vertical alignment on PI films. Therefore, the result of the computer simulation and the fact of LC vertical alignment on films suggest that the side chain is almost perpendicular to the main chain.

In order to investigate further the change of molecule conformation of the PI side chain, angle-resolved analysis XPS was introduced. Sampling depth is limited by inelastic scattering events, which are characterised by the inelastic mean free path of the photo-electrons. Since approximately 95% of the signal intensity is

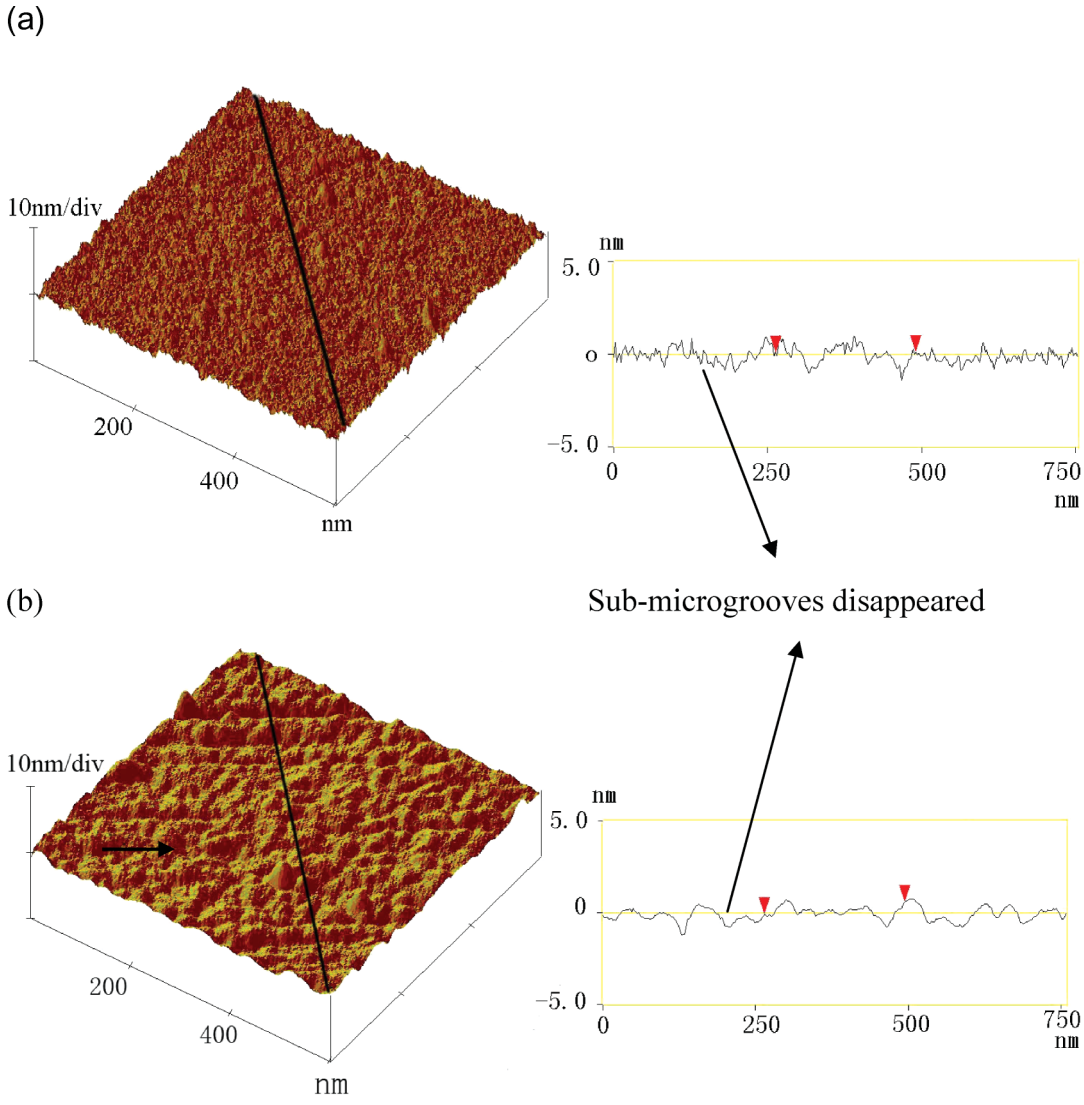

Figure 4. Atomic force microscope images and surface profiles of the (a) pristine polyimide and (b) rubbed polyimide. The arrow in each image denotes the rubbing direction.

Figure 5. The energy minimised structures of the polyimide with bulky side chain; the length of the side chain is 26.438 Å.

derived from a distance of 3λ within the solid, the sampling depth, d, as a function of the angle Θ of electron exit relative to the surface of the sample, that is, the take-off angle (TOA), is usually taken to be [27]

$$d = 3\lambda \sin \Theta. \quad (1)$$

The high-resolution C Is core-level photo-emission spectra of the pristine and rubbed PIs are shown in Figure 6. The component peak at 284.7 eV is attributed to carbon atom bonds from the aromatic rings and alkyl end group. The peaks at 286.1 and 288.7 eV are attributed to the carbon atoms singly bonded to oxygen C–O and the ester carbons O–C=O, respectively. The low-intensity peak (291.1 eV), which appears at higher binding energy, is the fingerprint of an energy loss of the electrons related to a π–π* shake-up transition process [28–30]. Such a transition is generally observed in polymer systems containing conjugated electrons. Figure 6(a) and (b) show the XPS spectra of C 1s at 60° TOA. Assuming that the inelastic mean

free path, λ, of the C Is photo-electrons in organic compounds is 2.7 nm [31], the sampling depth was calculated to be about 7 nm according to Equation (1). The results of XPS spectra show that the C/O/N atomic ratio was not obviously altered by rubbing, but the relative ratio of carbon after rubbing decreased slightly from 83.5% to 82.7%. Furthermore, from Table 2 it is clear that the relative ratio of carbon bonded to oxygen increased. This indicates that the non-polar alkyl group on the film surface decreased and was consistent with the foregoing result, which was that the surface free energy of PI films decreases after rubbing.

Table 2. Results of the peak separation of X-ray photo-electron spectroscope C 1s spectra.

	Atomic percentage (%)			
PI/take-off angle	C–C	C–O	C=O	Shake-up
Pristine PI/60°	64.6	21.3	12.9	1.2
Rubbed PI/60°	59.3	23.3	15.3	2.1
Pristine PI/10°	47.3	44.2	8.5	
Rubbed PI/10°	52.6	36.7	10.7	

Note: PI = polyimide.

Figure 6(c) and (d) present the XPS spectra with 10° TOA. According to Equation (1), the sampling depth was 1.4 nm. On the other hand, from Figure 5 it is seen that the length of the side chain of the PI is approximately 2.6 nm. As for the pristine PI, this suggests that the XPS spectra with 10° TOA only include information from the side chain. The disappearance of the nitrogen atomic signal in the XPS spectra with 10° TOA (Figure 7) can further prove that the signals of the side chain only are shown in Figure 6(c) and (d) because nitrogen atoms only exist in the macromolecules of the main chain. Compared with Figure 6(a) and (b), (c) and (d) show that the peak area of the C 1s spectrum at 288.7 eV (C=O) decreases remarkedly, while the shake up at 291 eV completely disappears. The change is consistent with the results that the sampling depth became so shallow that the XPS signals of the main chain disappeared in Figure 6(c). So it is concluded that the XPS spectra with 10° TOA only include signals from the side chain.

Since it is concluded that the XPS spectra with 10° TOA only include signals from the side chain, the XPS spectra with 10° TOA were analysed further. It can be

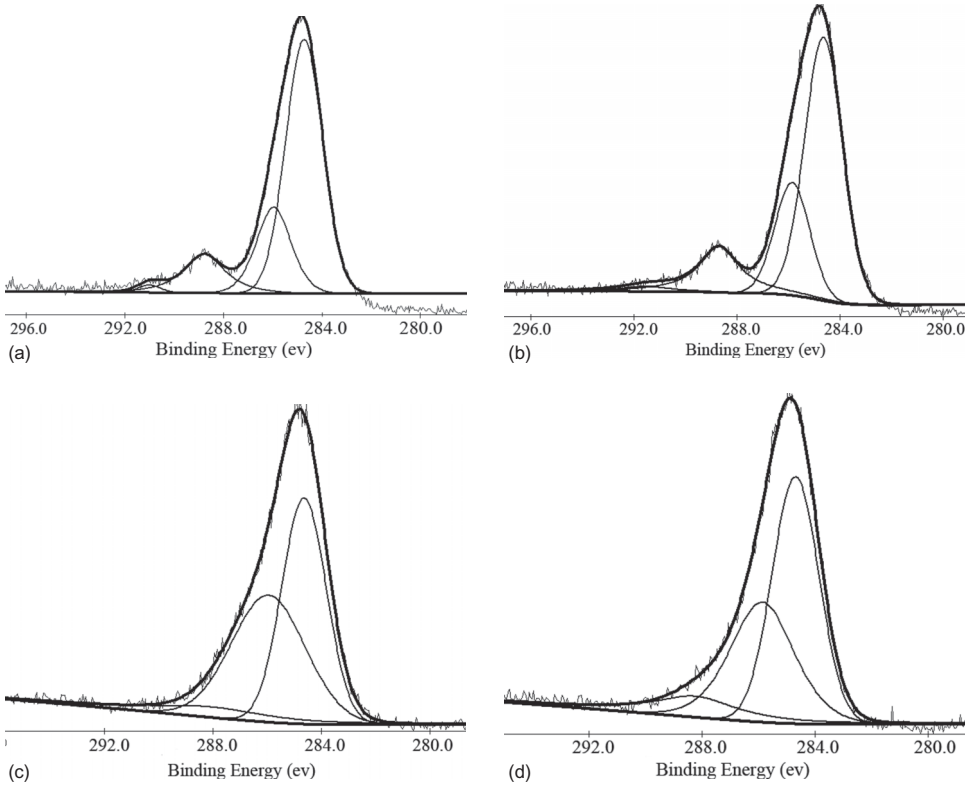

Figure 6. The curve-fitted C 1s spectra of: (a) rubbed polyimide with 60° take-off angle (TOA); (b) pristine polyimide with 60° TOA; (c) pristine polyimide with 10° TOA; (d) rubbed polyimide with 10° TOA.

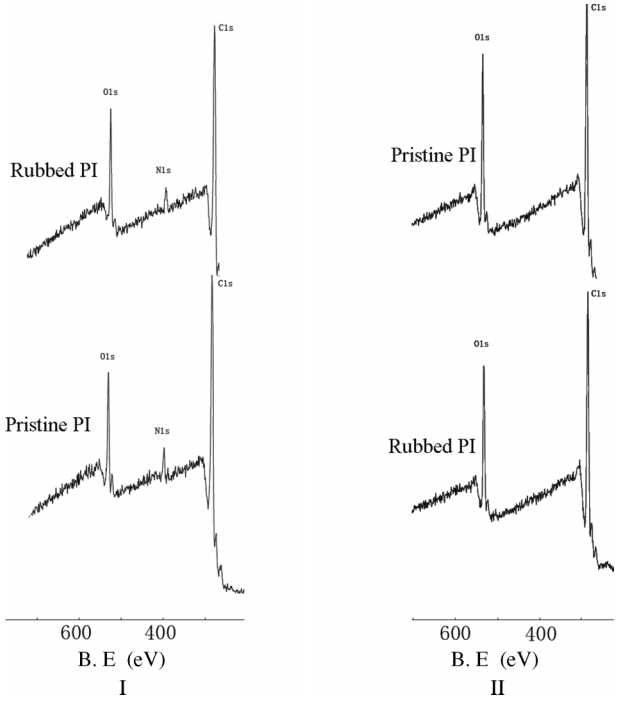

Figure 7. Survey of X-ray photo-electron spectra of 60° take-off angle (TOA) polyimide I and 10° TOA polyimide 2.

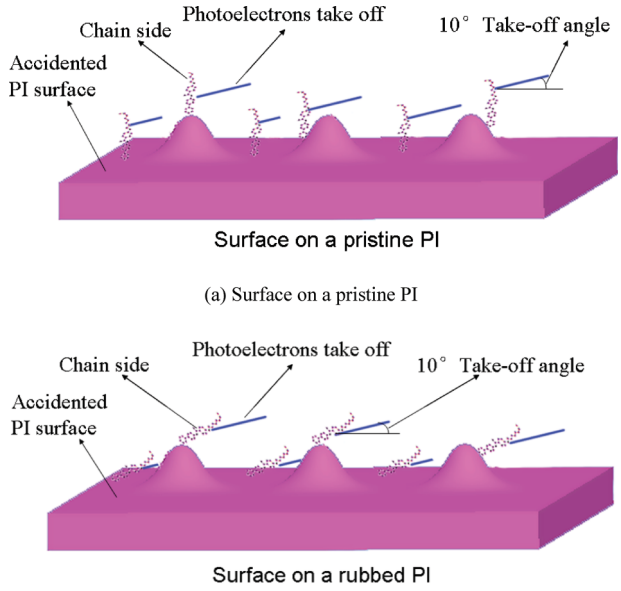

Figure 8. Schematic mechanism of the microscopic molecular reorientation of the polyimide surface layer (a) before rubbing and (b) after rubbing.

seen that the C 1s peak at 286.1 eV (C–O) of Figure 6(c) is stronger than that of (d). Furthermore, Table 2 also shows that the C–O percentage ratio decreases after the rubbing process. Meanwhile, it can be seen from Table 2 and Figure 6(c) and (d) that the percentage ratio of C=O obviously increased after rubbing. Why do XPS spectra with 10° TOA present an obvious decrease of the percentage ratio of C–O and increase of the percentage ratio of C=O? As mentioned above, surface roughness does not apparently change after rubbing. The reason for this is that the side chain of the PI falls down on the polymer surface. As shown in Figure 8(a), as the side chain is perpendicular to the PI surface before rubbing, the photo-electrons from the side chain emit and easily enter a photo-electron detector. On the other hand, since the side chain droops on the PI surface via rubbing (Figure 8(b)), after the photo-electrons emit, the accidented surface prevents the photo-electrons from entering the XPS detector. Therefore, the signal intensity and percentage ratio of C–O from the side chain decrease. The droop of the side chain results in the presence of a small C=O from the imide group in the XPS spectra with 10° TOA, so the C=O percentage ratio has a corresponding increase.

This was the first time that the XPS had been used for analysing the conformational change of the side chain of a polymer, and the conformational change could be detected owing to the special structure of the PI. First, the PI side chains possess C–O groups, which the main chain does not yet possess. Second, the three C–O groups from the side chain can induce sufficient signal intensity to be detected and analysed by XPS. Although NEXAFS, SFG and SHG have become effective methods for surface analysing, especially the conformational change in polymers, our study demonstrated that the traditional means of measurement, XPS, can also analyse qualitatively the molecular conformational change.

We investigated the change of surface energy, surface morphology and side chain conformation on a PI for designing an appropriate PI molecular structure to align vertically NLCs. It is clear that only the droop of the side chain on the PI can dominate the transition of LC alignment from homeotropic to planar on a PI layer. The result implies that the side chain conformation is the most elemental factor for NLC homeotropic alignment on a PI surface.

4. Conclusion

We designed a PI with a special side chain to investigate the different factors (surface energy, surface morphology and side chain conformation) correlating with the pretilt angle. It was found that neither surface energy nor surface morphology dominated the transition of LC alignment from homeotropic to planar on the PI layer. Moreover, the droop of the side chain after rubbing treatment was detected by XPS spectra. It was the first time that the XPS had been used successfully for

analysing the conformational change of the side chain of a polymer due to the special structure of the PI. Furthermore, it was concluded that the change of the side chain on the PIs was vital for the transition of the LC alignment from homeotropic to planar after a strong rubbing process. The result is helpful in understanding further the mechanism of vertical alignment for NLCs, and is helpful in the enhancement of NLC vertical alignment stability on a PI.

Acknowledgements

We would like to acknowledge the useful advice from Makoto Takeishi of Yamagata University. We would also like to thank Hong Cheng, Analytical and Testing Centre of Sichuan University, for her kind assistance in the XPS measurements. This work was supported by the National Natural Science Foundation of China (Grant No. 50973067), Fund from the State Key Laboratory of Polymer Materials Engineering (Sichuan University) and the project sponsored by the Scientific Research Foundation for the Returned Overseas Chinese Scholars, State Education Ministry, and Science (No. 20071108-18-12).

References

[1] Hoi-Sing, K.; Vladimir, G.C.; Hirokazu, T.; Haruyoshi, T. *J. Display Technol*. **2005**, *1*, 41–50.
[2] Dong-Hun, K.; Sang-Hoon, K.; Byoung-Yong, K.; Jong-Yeon, K.; Chul-Ho.; Young-Hwan, K. *Jpn. J. Appl. Phys.* **2007**, *46*, 6601–6603.
[3] Johan, H.; Theo, R.; Alan, E.R.; Roeland, J.M.N. *J. Mater. Chem.* **2006**, *16*, 1305–1314.
[4] Jeoung-Yeon, H.; Seung, H.L.; Seung, K.P.; Dae-Shik, S. *Jpn. J. Appl. Phys.* **2003**, *42*, 1713–1714.
[5] Zhibin, H.; Charles, R. *Appl. Phys. Lett.* **2005**, *86*, 011908.
[6] Sinha, P.S.; Wen, B.; Charles, R. *Appl. Phys. Lett*. **2001**, *79*, 2543–2545.
[7] Lee, K.W.; Paek, S.H.; Lien, A.; Durning, C.; Fukuro, H. *Macromolecules (Washington, DC, U. S.)*. **1996**, *29*, 8894–8899.
[8] Seo, D.S.; Kobayashi, S. *Liq. Cryst.* **2000**, *27*, 883–887.
[9] Newsome, C.J.; O'Neill, M. *J. Appl. Phys.* **2002**, *92*, 1752–1756.
[10] Seo, D.S. *J. Appl. Phys.* **1999**, *86*, 3594–3597.
[11] Jong-Woo, L.; Hee-Tak, K.; Shi-Joon, S.; Jung-Ki, P. *Synth. Met.* **2001**, *117*, 267–269.
[12] Paek, S.H.; Durning, C.J. *J. Appl. Phys.* **1998**, *83*, 1270–1280.
[13] Kiryong, H.; John, L.W. *Liq. Cryst*. **2004**, *31*, 753–757.
[14] Da-Ren, C.; Kuan-Yu, Y.; Li-Jen, C. *Appl. Phys. Lett.* **2006**, *88*, 133123.
[15] Da-Ren, C.; Li-Jen, C. *Langmuir* **2006**, *22*, 9403–9408.
[16] Takahiro, S.; Ken, I.; Hideo, T. *J. Phys. Chem.* **2001**, *105*, 9191–9195.
[17] Himali, D.J.; Min, H.Z.; Charles, R. *J. Chem. Phys.* **2006**, *125*, 064706.
[18] Jason, J.G.; Christopher, Y.L.; Gi, X.; Ian, K.M.; Dong, Z. *J. Am. Chem. Soc.* **2001**, *123*, 5768–5776.
[19] Oh-e, M.; Yokoyama, H.; Kim, D.S. *Phys. Rev. E Stat., Nonlinear, Soft Matter Phys.* **2004**, *69*, 051705.
[20] Jian, W.; Yinghan, W. *Chin. Chem. Lett.* **2008**, *19*, 59–362.
[21] Seo, D.S.; Kobayashi, S. *Appl. Phys. Lett.* **1992**, *61*, 2392–2394.
[22] Yoon, J.L.; Yong, W.K.; Jae, D.H. *Polym. Adv. Technol.* **2007**, *18*, 226–234.
[23] Ban, B.S.; Kim, Y.B. *J. Appl. Polym. Sci.* **1999**, *74*, 267–271.
[24] Boknam, C.; Seung, B.K.; Seung, W.L.; Sang, I.K.; Wooyoung, C.; Byeongdu, L. *Macromolecules (Washington, DC, U. S.)*. **2002**, *35*, 10119–10130.
[25] Mada, H.; Snoda, T. *Jpn. J. Appl. Phys.* **1993**, *32*, 1245–1247.
[26] Toney, M.S.; Russel, T.P.; Logan J.A.; Kikuchi, H.; Sands, J.M.; Kumar, S.K. *Nature (London U.K.)*. **1995**, *374*, 709–711.
[27] Quoc, T.L.; Pireaux, J.J.; Caudano, R. *J. Adhes. Sci. Technol.* **1997**, *11*, 735–751.
[28] Zhao, J.H.; Beng, K.T.; Peter, C.T. *J. Appl. Phys.* **2007**, *101*, 053301.
[29] Zeng, D.W.; Yung, K.C.; Xie, C.S. *Surf. Coat. Technol.* **2002**, *153*, 210–216.
[30] Pierre, L.; Frederic, B.; Jean-Jacques, P. *Surf. Sci. Spectra* **2005**, *12*, 121–126.
[31] Jin, H.K.; Kil, W.C.; Jin, K.K.; Chan, E.P.; Sung-Jin, U.; Bhanu, B.K. *J. Adhes. Sci. Technol.* **2004**, *18*, 1815–1831.